Low-Loss Passive Optical Waveguides Based on Photosensitive Poly(pentafluorostyrene-*co*-glycidyl methacrylate)

Claire Pitois, Sonia Vukmirovic, and Anders Hult*

Royal Institute of Technology, Department of Polymer Technology, S-100 44 Stockholm, Sweden

Dorothea Wiesmann

IBM Zurich Research Laboratory, CH-8803 Rüschlikon, Switzerland

Mats Robertsson

Ericsson Components AB, Unit MEST, S-164 81 Kista-Stockholm, Sweden

Received July 6, 1998; Revised Manuscript Received December 29, 1998

ABSTRACT: Low-loss optical waveguides have been fabricated from fluorinated copolymers designed to incorporate photochemical amplification based on acid catalysis. Core and cladding layers were made, for single-mode (SM) channel waveguides, from the poly(pentafluorostyrene-*co*-glycidyl methacrylate) copolymer series and, for multimode (MM) ridge waveguides, from poly(*tert*-butyl methacrylate-*co*-glycidyl methacrylate) as the cladding and poly(pentafluorostyrene-*co*-glycidyl methacrylate) as core layer. The reactivity ratios for PFS and GMA monomers have been measured to be r(PFS) = 0.38 ± 0.01 and r(GMA) = 0.89 ± 0.01 in free radical polymerization. Variation of the copolymer composition allowed precise control over the refractive index measured at 589, 633, 1320, and 1550 nm. These amorphous copolymers were photo-cross-linked by contact printing and developed by wet etching to produce high quality ridge waveguides with very smooth top surfaces. Low loss single-mode (SM) waveguides exhibit averaged losses over eight channel waveguides as low as 0.39 dB/cm at 1320 nm and 0.42 dB/cm at 1550 nm. Thermal properties have been examined and optical losses were measured after two different annealings at 200 and 250 °C for 1 h.

Introduction

The continual trend toward high transmission speed, data capacity, and data density in integrated circuits demands a solution to the bottleneck resulting from the limited data rate of electrical interconnects. One approach to this problem is the use of optical interconnection operating with polymer waveguides. This alternative has been widely reported[1,2] and shows advantages for large-system applications (a few centimeters to 1 m). It reduces electromagnetic interference and has lower power requirements. Optical polymer waveguides are potentially useful for low-level hierarchies, such as board-level or backplane-level interconnections, and flexible manufacturing techniques have been reported that can be applied on a large variety of substrates.

Polymer materials have tailorable optical properties (such as refractive index and optical losses) and exhibit excellent mechanical and physical properties that are essential for making reliable optical devices. Nevertheless, many polymers have two disadvantages. They have limited thermal stability of optical losses (lower than 200 °C), except for polyimides, which exhibit a decrease of only 5% after annealing at 300 °C for 1 h,[3,4] and polysiloxanes, which had propagation losses that remained unchanged after heating at 200 °C for 30 min.[5] Second, polymers exhibit high absorption or high optical losses compared to silica fibers in the range of wavelengths used for telecommunication transmission, the near-infrared (NIR). The loss can be limited by shifting the high absorption signal toward longer wavelengths by replacing hydrogen atoms with heavier atoms such as deuterium or halogens, essentially chlorine or fluorine.

Low-loss, fluorinated polyimide waveguides fabricated either by photolithography followed by reactive ion etching (RIE)[4] or by electron-beam lithography[6] have shown losses of 0.3 dB/cm at 1300 nm. Deuterated polysiloxane single-mode (SM) waveguides have reached losses as low as 0.17 dB/cm at 1310 nm and 0.43 dB/cm at 1550 nm.[7] Other methods such as photolocking,[8] selective photopolymerization,[9] injection molding,[10] or standard photolithography with wet etching[11,12] have been investigated to reduce either the number of processing steps or the etching time required to produce the guides. The photosensitive epoxy material reported by J. M. Trewhella et al.[12] showed both low loss and reasonably good thermal stability over 200 °C. However, the high refractive index (around 1.598) of the fully epoxidized Novolac system used in that work can induce extra losses due to back-reflection when directly coupled to a silica optical fiber with a refractive index of 1.46 at 633 nm.

We report the preparation and characterization of low-loss polymer waveguides made from fluorinated copolymers. They exhibit refractive indexes close to that of silica optical fibers, and are manufactured by conventional contact-printing photolithography. Fluorinated copolymers were produced from pentafluorostyrene (PFS) and glycidyl methacrylate (GMA), shown in Figure 3. The polymerization procedure is described and reactivity ratio measurements are presented. When mixed with an acid-generating photoinitiator,[13] these copolymer films undergo cross-linking by photochemical amplification to generate a latent image of a photomask.[14] This image can be developed by wet etching to

* To whom correspondence should be addressed.

10.1021/ma981057x CCC: $18.00
Published on Web 04/06/1999

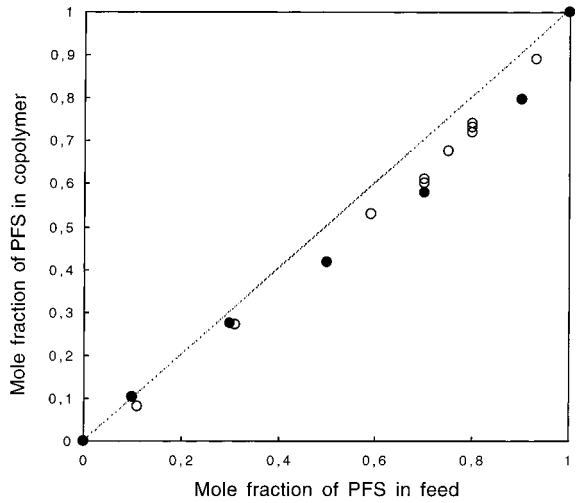

Figure 1. Copolymer composition vs monomer feed of PFS and GMA at low conversion (●), and high conversion (○).

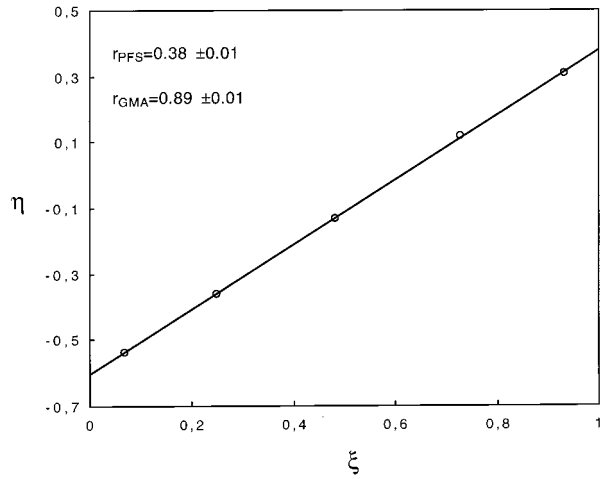

Figure 2. Data of PFS/GMA copolymerization system plotted according to the Kelen−Tüdös equation.

produce very smooth top-surfaces in the relief image. Both single-mode (SM) and multimode (MM) waveguides have been made, and low losses have been obtained at 1320 and 1550 nm. The thermal stability of the materials has been studied, and changes in optical loss as a function of annealings were measured.

Results and Discussion

Copolymerization. Monomer reactivity ratios have been studied in order to better understand the solution free radical copolymerization of PFS with GMA. Table 1 shows the experimental conditions. The polymerization was driven to low conversion (<9%) to satisfy the differential copolymerization equation. The average composition of the copolymers was determined by ^{13}C NMR. The copolymer composition curves at both low and high conversions are shown in Figure 1. A Kelen−Tüdös plot[21] is shown in Figure 2, and the corresponding reactivity ratios are $r_1 = 0.89 \pm 0.01$ for GMA, and $r_2 = 0.38 \pm 0.01$ for PFS. The value of r_1 is close to unity indicating that the propagation species GMA* shows no substantial preference for either GMA or PFS monomers. The relative rates of monomer consumption are therefore dependent only by the initial monomer concentrations in the feed, as illustrated in Figure 1 for the low concentrations of PFS in the monomer feed mixture. The value of r_2 reveals a slight preference for the propagation species PFS* for GMA monomers. The lower reactivity of PFS monomers is also evidenced by the decreasing yield and molecular weight of the copolymer with increasing PFS in the feed (Table 1).

Monomer reactivity can also be interpreted in terms of monomer resonance stability in copolymerization (Q) and polarity factor (e), which were introduced by Alfrey and Price.[15] The Q and e values for PFS were calculated from the reactivity ratios, according to the following equations, with the indices 1 standing for GMA and 2 for PFS. Considering the values $Q_1 = 0.78$ and $e_1 = -0.02$[16]

$$e_2 = e_1 \pm [-\ln(r_1 r_2)]^{1/2} \quad (1)$$

$$Q_2 = Q_1/r_1 \exp[-e_1(e_1 - e_2)] \quad (2)$$

The calculated values for PFS are $Q_2 = 0.85$ and $e_2 = 1.02$. These values are compared with those reported in the literature[17] in Table 2. It has been recognized that there is a linear relationship between vinyl monomer reactivity and NMR chemical shifts and between monomer e values and chemical shifts.[18a−g] Herman and Teyssié have suggested that the parameter e for substituted styrene monomers may be estimated from the chemical shift of the β-carbon according to

$$e = \frac{\delta(C_\beta)(\text{ppm/TMS}) - 115.5}{3.5} \quad (3)$$

The application of eq 3 to the $\delta(C_\beta)$ of PFS (121.4 ppm) gives an estimated value of $e = 1.68$, which is closer to that calculated from the reactivity ratios determined in this work.

The rather high polarity of PFS ($e = 1.02$) results in rather low reactivity toward electrophilic radicals (PFS*) and rather high reactivity toward more nucleophilic radicals (GMA*). This is consistent with our observations that $k_{22} < k_{21}$ ($r_2 = 0.38$) and $k_{12} > k_{11}$ ($r_1 = 0.89$). The reactivity of the polymer radical is known to contribute more strongly to the propagation rate (k_p) than the reactivity of the monomer. It is therefore expected to be more difficult for the electrophilic radical PFS* to add to the electron-deficient PFS monomer than to the more electron-rich GMA monomer. So, the experimental tendency toward alternation may be due to the significant polarity difference between both monomers ($e_1 = -0.02$, $e_2 = 1.02$).

Lithographic Evaluation and Waveguide Fabrication. The negative photoresists elaborated in this study have been designed to contain photochemical amplification based on acid catalysis. Cationic rather than radical photochemistry was preferred because it is not inhibited by atmospheric oxygen. Systems incorporating chemical amplification were first introduced by Ito et al.[14a−d] to circumvent sensitivity limitations in photoresists. Another advantage of these systems is the low amount of photoinitiator necessary to photopattern images, thus minimizing optical losses induced by the photoinitiator.

As shown in Figure 3, the nature of photoinitiators was chosen depending on its solubility in the various copolymer compositions. Arylsulfonium hexafluoroantimonate salts did not phase separate in P(PFS−GMA) films of PFS at concentrations up to 80 mol %. The nonionic *N*-perfluorobenzenesulfonyloxynaphthalimide

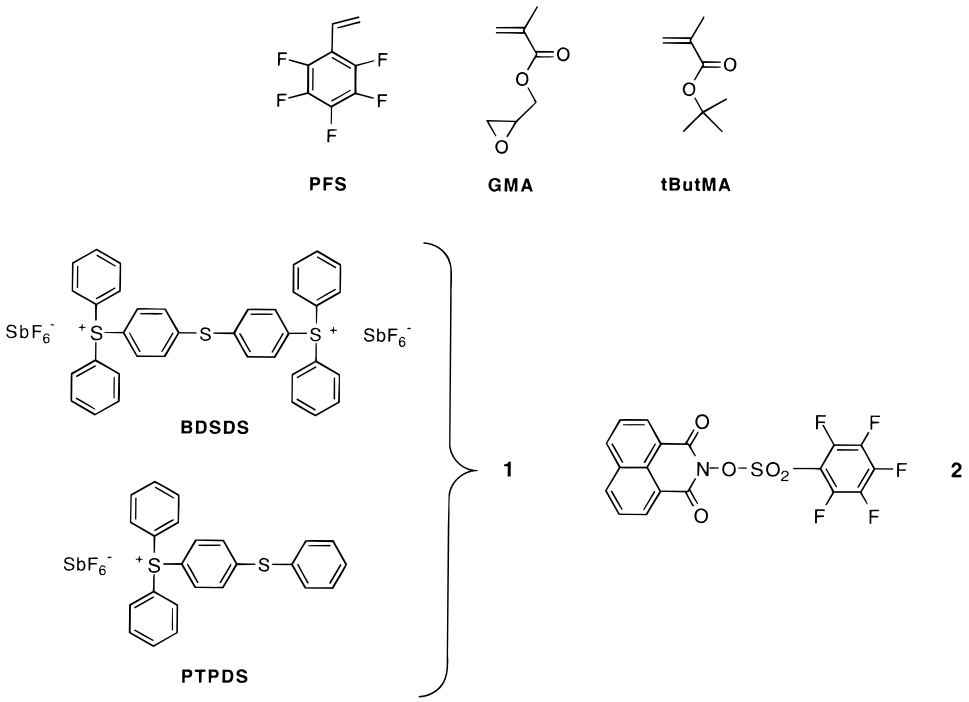

Figure 3. Monomers used: pentafluorostyrene (PFS), glycidyl methacrylate (GMA), and *tert*-butyl methacrylate (tButMA). Acid-generated photoinitiators: (1) mixture of 4,4-bis(diphenylsulfonio)-diphenylsulfide hexafluoroantimonate (BDSDS), and 4,4-(phenylthio)phenyldiphenylsulfonium hexafluoroantimonate (PTPDS); (2) *N*-perfluorobenzenesulfonyloxynaphthalimide.

Table 1. Radical Copolymerization of Pentafluorostyrene (PFS) and Glycidyl Methacrylate (GMA)[a]

polymer no.	PFS feed, mol %	GMA feed, mol %	time	yield, mol %	mole fraction of PFS in copolymer	$\bar{M}_n$[b]	PD[c]
P1	10	90	15[d]	8.90	10.3		
P2	30	70	15[d]	4.57	27.4		
P3	50	50	20[d]	3.93	42.1		
P4	70	30	20[d]	2.74	58.0		
P5	90	10	20[d]	2.57	79.9		
P6	11	89	10[e]	93.1	8.0	53 700	1.75
P7	31	69	20[e]	70.4	27.0	51 400	1.71
P8	59	61	20[e]	66.3	53.0	27 000	1.75
P9	70	30	20[e]	56.5	60.0	29 900	1.68
P10	75	25	20[e]	51.8	67.7	35 400	1.72
P11	80	20	20[e]	50.9	73.2	30 800	1.73
P12	93	7	20[e]	50.5	89.0	28 400	1.66

[a] [AIBN] = 0.2 wt %, temp = 70 °C, in toluene. [b] Number-average molecular weight. [c] Polydispersity. [d] Minutes. [e] Hours.

Table 2. Copolymerization Parameters *Q* and E for PFS

M_1	M_2	Q_{PFS}	e_{PFS}	ref
GMA	PFS	0.85	1.02	this work
styrene	PFS	0.69	0.74	20
methyl methacrylate	PFS	0.87	0.75	20

acid generator was preferred for copolymer systems of higher molar ratios of PFS (e.g., polymers used for cladding layer in SM waveguides). This is due to both the initiator nonionic nature and the pentafluorophenyl group which enhanced solubility in the copolymer matrix.

The photolysis of triarylsulfonium salts generates strong Brönsted acids that initiate cationic polymerization of the oxirane residues on the GMA monomers. This reaction can be monitored by IR spectroscopy by the appearance of the hydroxyl stretching band at 3500 cm^{-1} and the decrease of the oxirane ring vibrations at 910 and 848 cm^{-1}. This cross-linking reaction gives rise to an insoluble three-dimensional network in the resist exposed areas.

Lithographic evaluation was performed on the polymers intended to be the core material of the waveguides. The contrast curves for P11 and P8 of 10 μm thick films (multimode) containing 0.7 w/w to copolymer of onium salts are given in Figure 4. These samples coated on quartz wafers by the procedure described in the Experimental Section (Waveguide Fabrication). UV irradiation was applied through a 313 nm narrow-band filter (peak wavelength, 313 nm; bandwidth, 11 nm) through the back of the quartz wafers. The plot in Figure 4 represents the remaining film thickness after wet-development vs the log of the exposure dose, keeping the process conditions constant. Sensitivities taken at 50% of the gel dose are 17.8 and 14.1 mJ/cm^2 for P11 and P8, respectively. The copolymers have very similar molecular weights and polydispersities, and their 10 °C difference in glass transition temperature has been taken into account in the postbaking conditions in order to afford the same mobility in both polymers. Therefore the increase of 21% in sensitivity from P11 to P8 is ascribed to the increase of almost 20 mol % of the epoxy groups in the copolymer structure. The contrast of P11 of 4 μm thick films (single-mode) containing 0.7 w/w to copolymer of onium salts is 1.4, slightly lower than of

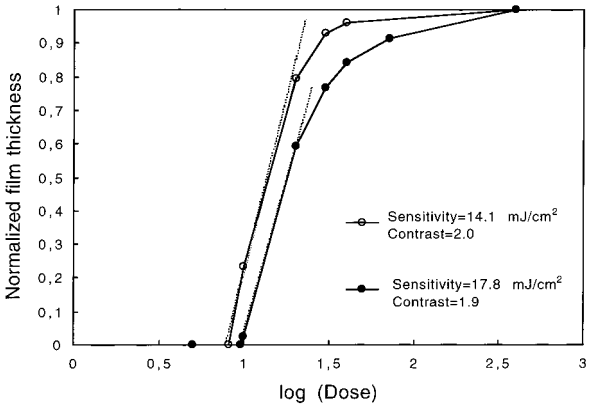

Figure 4. Sensitivity curve at 313 nm for both wet-developed systems: P8 (○), and P11 (●) processed according to the MM procedure for core layers described in the Experimental Section.

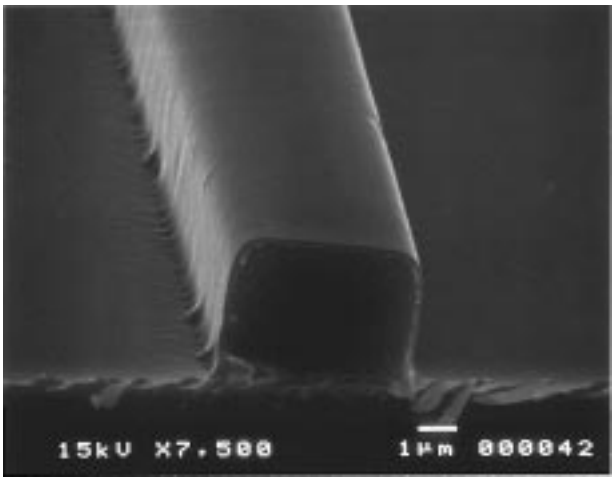

Figure 5. SEM micrograph depicting a single-mode core optical waveguide of P11 containing 0.7 wt % of onium salts (photoinitiator **1**). This ridge waveguide has a cross section of 5×4 μm and was patterned on oxidized silicon substrate.

the MM analogue (almost 2). However, this contrast is sufficient to lead to vertical sidewalls in the relief image generated in this polymer, as demonstrated in Figure 5. In this micrograph, the unoptimized process conditions were the same as those used to characterize the contrast, except for the exposure dose which was set at 200 mJ/cm^2. Very smooth top surfaces were generated after wet development. Nevertheless, the side walls of the waveguides present some vertical corrugations, which curve into the base of the waveguides. We believe that optimizing all the processing steps and using spray rather than immersion development can reduce these irregularities.

Development is one of the most delicate and crucial stages in photolithography. To generate smooth and well-defined structures, two issues have to be examined: the choice of polymer type and the choice of the solvents.

One of the factors influencing the dissolution characteristics of polymers is their free volume. Ouano et al.[19] have clearly demonstrated the extensive cracking dissolution behavior of atactic poly(methyl methacrylate) and the extensive swelling behavior of polystyrene. Substantial cracks may be difficult to remove by annealing and may reappear when spin-coating a cover layer, whereas substantial swelling would induce severe distortions in the waveguide such as the typical snake-like formation. Concerning fluorinated copolymers, we previously experienced cracking behavior for the random acrylate system poly(pentafluorophenyl methacrylate-*co*-GMA), which made crack-free waveguides difficult to reproduce. Therefore we chose to combine styrenic and methacrylic structures in the P(PFS−GMA) copolymers, with which cracks or swelling were minimized and the line width (resolution) of the waveguide core was measured by SEM to be ±2% the size of the photomask line.

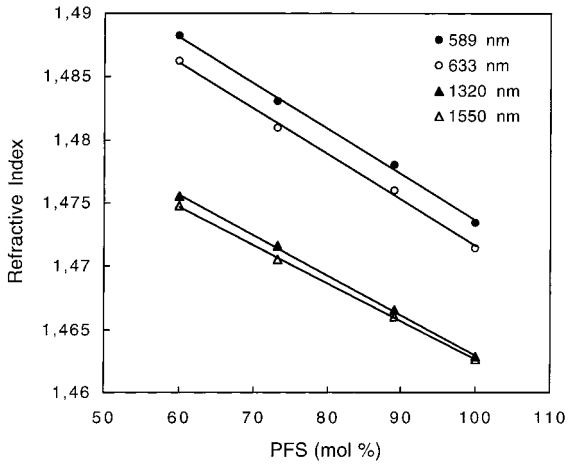

Figure 6. Refractive index of P(PFS−GMA) comonomers vs PFS amount, measured at four different wavelengths.

The second factor is of course the judicious selection of solvents employed in the development procedure. We applied the basic concept described by November et al.[22] to this selection. A succession of solutions with less and less solubility for the polymer was tested. The developer should not lead to pattern distortion due to swelling, and should rapidly remove the unexposed areas. We thus chose as the developer solution a mixture of good and poor solvents, 2,4-pentanedione and 1-butoxybutane, respectively. By varying their concentration, we were able to adjust the solubility toward the polymer. These solvents are reasonably miscible and present good kinetic behaviors or a short time to dissolve away the polymer, as judged by their low molar volume: the calculated values are 93 cm^3/mol for 2,4-pentanedione and 112 cm^3/mol for 1-butoxybutane. The concentration of each solvent was also adjusted in function of the thickness of the polymer film to be developed. The last rinse was chosen to be diethyl ether, which is a rather strong nonsolvent and therefore slightly shrinks the final features.

Optical Characterization. Efficient coupling between waveguides and other devices (fibers, lasers, etc.), requires careful control and matching of both the physical size and the numerical aperture of the waveguides. The physical size is adjusted by the fabrication process, whereas the numerical aperture is governed by the relative refractive indexes of the core and cladding polymers. The refractive index of P(PFS−GMA) copolymers vs the amount of PFS is plotted in Figure 6 for four selected wavelengths (589, 633, 1320, and 1550 nm). Before index measurement, the copolymer films were cured according to the SM process described in the Experimental Section. We focused on establishing a copolymer ratio that has a refractive index similar to that of SM glass optical fibers ($n = 1.46$ at 633 nm). The refractive index at 589 nm for the P(PFS−GMA) core varies between 1.471 and 1.486, as PFS content

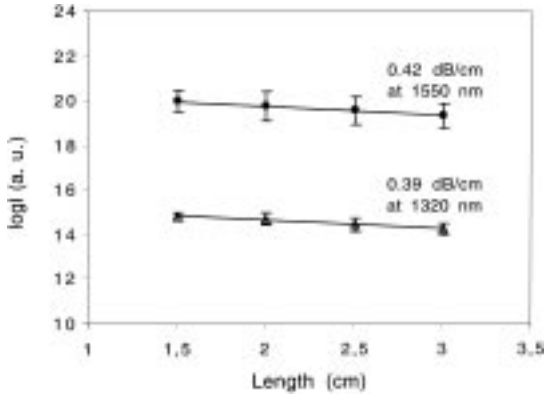

Figure 7. Optical loss measured at 1320 and 1550 nm in SM waveguides by the cut-back method.

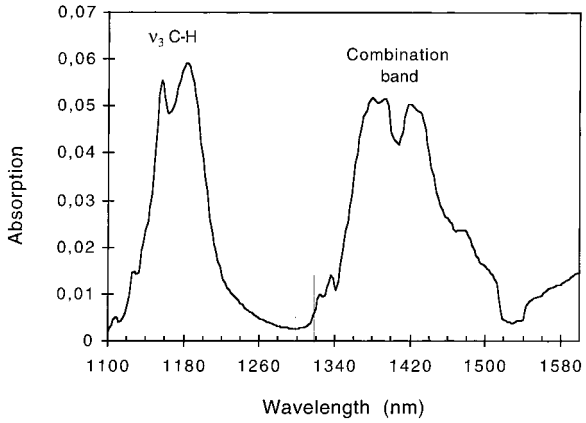

Figure 8. Near-infrared absorption spectrum of P11 in solution with chloroform-*d*.

varies from 87 to 60 mol %. The rather small index difference between the polymer waveguide and the glass fiber is designed to minimize the back-reflection from the waveguide-fiber interface. As seen in Figure 6, the refractive index of the copolymer is the molar average of those of the monomers PFS and GMA, indicating linearity of the refractive index with copolymer composition. The birefringence of these copolymers does not exceed 4×10^{-4} at 633 nm, and therefore, one may assume that the effects of morphology on the refractive index are negligible.

From Figure 6 we were able to determine the proper physical shapes of each of the waveguide layers in order to generate single mode channel waveguides at 1320 and 1550 nm. We calculated the maximum channel dimensions for single-mode operation with the commercially available software Selene-Pro, which is based on a finite element analysis. We found that the waveguides made on thermally grown SiO_2 as bottom cladding, with P11 as the core material and P12 as the top cladding are single-mode at 1320 nm if the bottom and top claddings are 7 and 5 μm respectively and if the core width and height are chosen as 5 and 4 μm, respectively.

Optical losses have been measured in such SM channel waveguides at 1320 and 1550 nm. The logarithm of the optical throughput vs length is shown in Figure 7. Each point on this graph is the intensity average over eight adjacent waveguides with the same cross-section dimension (the core is 4 μm thick over 5 μm wide). The losses determined from the slope amount to 0.39 dB/cm at 1320 nm and 0.42 dB/cm at 1550 nm. The standard deviation is 0.09 dB/cm for both measurements; this rather high value can be explained by the spatially varying roughness of the diced facets.

The factors influencing the observed losses are of intrinsic and extrinsic origins. The intrinsic loss is likely to be dominated by the absorption of the C−H and O−H overtone stretches and by combinations of overtone and deformation. Inhomogeneities formed during polymerization may also raise intrinsic losses. Nevertheless, this contribution is minor considering the small difference in reactivity ratios between GMA and PFS given in the Copolymerization section. We believe that the optical losses at 1300 and 1310 nm are significantly lower than those at 1320 nm as illustrated by the NIR absorption spectrum of P11 in deuterated chloroform shown in Figure 8. However, to determine quantitatively the intrinsic loss of the polymers, measurements have to be performed on cross-linked polymer films with a more sensitive technique than transmission spectroscopy, e.g., photothermal deflection spectroscopy. Most of the extrinsic losses originate from scattering are presumably due to side-wall irregularities of the waveguides as illustrated in Figure 5. Further investigations concerning the quantitative analysis of the origin of optical loss will be the subject of our next studies.

Thermal Analysis. The glass transition temperatures (T_g) for P(PFS−GMA) polymers of similar molecular weights were found to vary with composition. The T_g increased linearly from 82 to 97 °C as the mole percent of PFS increased from 53 to 90 in the copolymers. Aromatic groups tend to raise the T_g due to intramolecular interactions (π-electron conjugation) which stiffen the main chain of the polymer.[20a] More experimental investigations have to be done to determine the T_g of cross-linked thin films (5−10 μm) processed by the procedure used for waveguide fabrication. Nevertheless, the maximum T_g values for P(PFS−GMA) can be reasonably accurately predicted using the theoretical formula of DiBenedetto,[20b] and assuming that all epoxy groups undergo cross-linking during the process. This assumption is unlikely to be achieved; therefore, the real T_g of the cross-linked films has to be found between the T_g of un-cross-linked films and the calculated maximum T_g of cross-linked films. These calculated values are between 105 and 110 °C for 10−47 mol % of GMA in the copolymers.

The TGA curves exhibit significant improvement of the thermal stability with increasing PFS in the polymers, as seen in Figure 9. Typically, the temperature of initial decomposition is 360 °C for the present system, compared to 280 °C for poly(methyl methacrylate),[20c] 327 °C for polystyrene,[20c] and 400 °C for polyimide or polysiloxane[7] under nitrogen atmosphere.

The most important issue is the retention of low optical loss upon thermal treatment. We thus annealed a series of eight SM channel waveguides at 200 °C for 1 h under nitrogen, and observed, on average, an increase of 0.33 ± 0.1 dB/cm at 1550 nm, raising the total waveguide losses from 0.42 to 0.75 dB/cm. Annealing at 250 °C for 1 h under nitrogen results in an average increase of 0.8 ± 0.3 and 0.53 dB/cm for the best waveguides.

Conclusion

Low-loss channel optical waveguides have been fabricated for 1320 and 1550 nm that should have losses lower than 0.39 dB/cm at 1310 nm according to the NIR

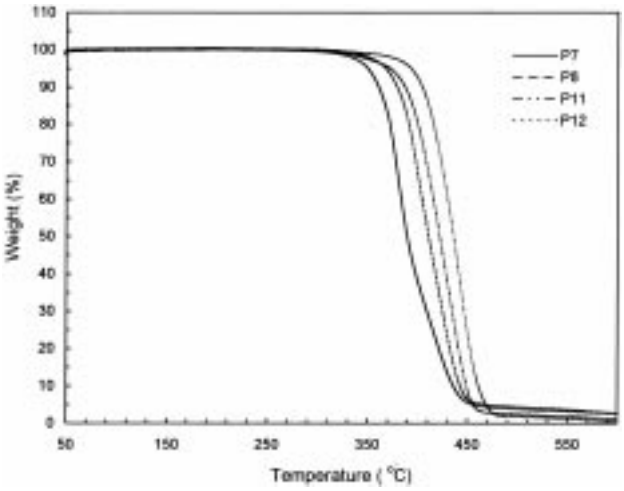

Figure 9. Influence of the copolymer composition on the thermal stability measured by TGA.

absorption spectrum. The combination of both styrenic, pentafluorostyrene (PFS), and methacrylic monomers, glycidyl methacrylate (GMA), in the copolymer structure provides good image retention after development of the cross-linked network (e.g. $\pm 0.1\mu$m of a 5 μm photomask line width). The refractive index of P(PFS-*co*-GMA) is decreased with increase of the PFS content due to both the lower molar polarization and the higher molar volume of PFS compared to GMA monomer. Measurement of the monomer reactivity ratios and calculation of the monomer polar factor indicate a tendency to alternation in free radical polymerization. Optical losses were observed to increase to 0.75 dB/cm at 1550 nm after annealing at 200 °C for 1 h under nitrogen atmosphere.

Experimental Section

Materials and Chemical Measurements. Pentafluorostyrene (PFS) was purchased from Fluorochem Limited, *tert*-butyl methacrylate (tButMA) was supplied by Polysciences Inc. (Warrington, PA) and glycidyl methacrylate (GMA) was purchased from Aldrich. Inhibitors were removed from tButMA and GMA on an aluminum oxide (neutral) column. All solvents were distilled before used. 2,2′-Azobis(isobutyronotrile) (AIBN), freshly recrystallized, was used as free-radical initiator. Copolymers were obtained by free-radical polymerization of dilute monomer solutions.

Chemical measurements of the copolymers synthesized were carried out by ^{1}H or ^{13}C NMR at 400 MHz in deuterated chloroform on a Bruker AC-400 spectrometer. Chemical shifts, δ, are given in ppm relative to TMS; solvent and internal standard are given in parentheses. Quantitative ^{13}C NMR spectra were obtained with gated decoupling without the nuclear Overhauser effect. The samples were prepared at 30 wt % polymer in $CDCl_3$ and were scanned 5000 times at a relaxation time of 10 s. FT-IR spectroscopy was performed with a Perkin-Elmer 1760X. The molecular weight distributions were determined by size exclusion chromatography (SEC). The copolymers were dissolved (4 mg in 1 mL of chloroform) and filtered before use (0.5 mm Teflon membrane). Two columns in series (PLgel-5-mm-MIXED-C) with a linear molecular weight range between 2×10^2 and 3×10^6 were used. Linear polystyrene was used as the calibration standard.

Thermal analysis was performed on a Perkin-Elmer DSC7 differential scanning calorimeter, calibrated according to standard procedure, at a heating rate of 10 °C min^{-1} under nitrogen. Thermal degradation was studied by thermogravimetric analysis (TGA) using a Mettler Toledo TGA/SDA 851^e measuring the mass loss in a heating scan from 40 to 600 °C at a rate of 10 °C min^{-1} with a nitrogen gas flow of 50 mL/min.

The photoinititors used for lithography were either the commercially available mixture of aryl sulfonium hexafluoroantimonates (also called UVI 6974 from Union-Carbide) or *N*-perfluorobenzenesulfonyloxynaphthalimide (Figure 3).

Free Radical Copolymerization of Poly(pentafluorostyrene-*co*-glycidyl methacrylate), P(PFS−GMA). Copolymers of pentafluorostyrene (PFS) and glycidyl methacrylate (GMA) were prepared with the monomer feed ratios (PFS/GMA) given in Table 1. Freshly distilled PFS (28 g, 144.3 mmol), GMA (8.78 g, 61.8 mmol), and AIBN (0.0737 g, 0.449 mmol) were mixed in toluene (112 mL). The flask was sealed with a rubber septum and deaerated by three freeze−pump−thaw cycles. The resulting solution was heated at 70 °C for 20 h under argon, and the formed polymer was precipitated into cold hexane (4 L) and dried. The resulting white polymer (20.2 g) was dissolved in dichloromethane and reprecipitated into cold hexane: this procedure was repeated three times.

Yield: 56.5%.

^{13}C NMR ($CDCl_3$, TMS): δ 175 (C═O), 146.8 to 136.1 (C−F), 115.5 ($C_{aromatic}$ in PFS), 65.8 (O−$\underline{C}H_2$−CH<), 49.6 to 38 (−CH_2− in PFS, −CH_2− in GMA, and $\underline{C}$ epoxy group in GMA), 31 (−CH< in PFS), 19 (−CH_3 in GMA).

IR (KBr, cm^{-1}): ν(C═O) = 1734, ν($C_{aromatic}$) = 1524 and 1502, ν(C−O epoxy) = 1254.

Free Radical Copolymerization of Poly(*tert*-butyl methacrylate-*co*-glycidyl methacrylate), P(tButMA−GMA). A series of copolymers of *tert*-butyl methacrylate (tButMA) and GMA was obtained by varying the monomer feed ratios (tButMA/GMA) in mole percent: 80/20, 70/30, 62/38, 60/40, 50/50, and 30/70.

tButMA (21 g, 147.9 mmol) and GMA (9 g, 63.4 mmol) were mixed with AIBN (0.0903 g, 0.55 mmol) in toluene (99.2 mL). The polymerization was carried out by the same procedure as described for P(PFS−GMA).

Yield: 95%.

The molecular weights ($\bar{M}_n$) were from 35 000 to 47 000, and the polydispersity (PD) from 2.2 to 2.5.

^{1}H NMR ($CDCl_3$, TMS): δ 4.26 and 3.84 (m, each 1H, O−$C\underline{H}_2$−CH<), 3.20 (m, 1H, −CH<), 2.82 and 2.62 (m, each 1H, −$\underline{C}H_2$− in epoxy), 1.41 (s, 9H, *tert*-butyl).

IR (KBr, cm^{-1}): ν(C═O) = 1724, ν(*tert*-butyl) = 1368, ν(C−O epoxy) = 1253.

Reactivity Ratio Determination. Monomer reactivity ratios for PFS and GMA were determined by the improved linear graphic method of Kelen and Tüdös,[21] based on the differential copolymer composition equation. Copolymer compositions were obtained by ^{13}C NMR.

Resist Formulation. Solutions were prepared by dissolving the photoinitiator and copolymers into cyclopentanone (30−50% wt/wt). For all the copolymers, except for P(PFS−GMA) having a PFS content greater than 80 mol %, the onium salt used for these experiments was a commercially available mixture of aryl sulfonium hexafluoroantimonates (**1** in Figure 3), which absorbs significantly at 313 nm. Its concentration in the polymer mixture was 0.5 wt % (vs polymer weight) for 10 μm thick films and 0.7 wt % for 4 to 5 μm thick films. For the most fluorinated copolymers (PFS > 80 mol %) constituting some of the cladding layers in the waveguides, the chosen photoinitiator was *N*-perfluorobenzenesulfonyloxynaphthalimide, which was kindly supplied by H. Ito (**2** in Figure 3). This photoinitiator absorbs mostly at 334 nm and was used at 1 wt % in the polymer solution for 7 μm thick films. All the solutions were filtered through 0.5 and 0.2 μm Teflon membrane filters before spin casting.

Waveguide Fabrication. Buried waveguides were fabricated by standard photolithographic technique using contact printing. Single mode (SM) and multimode (MM) waveguides were fabricated onto 4 in. silicon wafers according to the following procedure.

A low refractive index resist solution (e.g., P(PFS−GMA) for SM and MM or P(tButMA−GMA) for MM) was spun onto the silicon plate to give a 7−10 μm thick cladding layer. After being baked at 100 °C for 5 min on a hot plate, the film was UV-exposed under a Hg−Xe high-pressure lamp and post-baked at 130 °C for 30 min. The core of the waveguides was a

higher refractive index P(PFS−GMA) polymer spin-coated on top of the bottom cladding to form a 4 μm thick film for SM or 10 μm thick film for MM waveguides. The layer was baked at 130 °C for 1 min and patterned through a negative photomask by vacuum contact printing using a SUSS MA 56 production mask aligner having a line/space resolution of 0.4 μm at 300 nm. After postbaking took place for 30 min at 35 °C above the polymer glass transition temperature, the film was developed in dip mode using solvent combinations corresponding to the methodology described by November et al.[22] After being dipped for 30 s in a developer of 2,4-pentanedione and 1-butoxybutane (38/62 vol % for SM and 50/50 vol % for MM), the sample was then rinsed for 20 s in a solution of 33 vol % of 2, 4-pentanedione and 66 vol % of 1-butoxybutane and for 15 s in a bath of diethyl ether. The pattern was dried in air at 130 °C for 30 min to remove residual swelling. Resolution and image quality were determined by examining developed patterns with a JEOL Model JSM-5400 scanning electron microscope (SEM), with an accelerating voltage of 15 kV. Finally, the top cladding solution (identical to the bottom cladding solution) was spin-coated, dried at 100 °C for 15 min, UV-exposed, and postbaked at 100 °C for 30 min.

Optical Measurements. Refractive indices were measured at room temperature (19 to 22 °C) using three different methods depending on the wavelength. (i) At 633 and 1550 nm indices were measured by the well-known prism coupling technique[23] on 4 in. slab waveguides. Two identical prisms with a refractive index of 1.87 were pressed against the thin film of lower refractive index in order to couple light in and out. For certain angles of incidence the light is guided inside the slab waveguide and gives rise to a signal at the InGaAs-detector behind the second-outcoupling-prism. From these angles we determined the refractive index and the thickness of the polymer film. (ii) At 589 nm the refractive index was measured using a Carl Zeiss Abbe-refractometer. (iii) At 1320 nm the values were deduced from coupling the interference fringes in absorption spectra to the refractive index value obtained with the Abbe-refractometer.[24] This method actually leads to the refractive index dispersion from the UV to the NIR. The UV−vis−NIR absorption spectra were recorded on a Perkin-Elmer Lambda 9 spectrophotometer (speed 60 nm min^{-1}, slit width 2 nm). The spectra were recorded in reflection mode with an 6° angle of incidence in the polymeric film. The refractive index values obtained by this method at 633 and 1550 nm were verified as identical to those measured by method i.

The IR absorption spectrum in Figure 8 was obtained using a Fourier transform infrared spectrophotometer Perkin-Elmer 1760X. The polymer P11 was dissolved at 0.005 mol/L in deuterated chloroform. Quartz cells of 5 cm path length were used.

Optical losses of the channel waveguides were determined by the cut-back method, which consists of optical throughput measurements for different waveguide lengths. Light at 1550 nm from a tunable Photonetics laser or at 1320 nm from an HP Fabry Perot laser was coupled into the channel waveguides with a lensed fiber. On the output side a multimode fiber was connected to an InGaAs detector. The channel waveguides were cut back either by scribing and cleaving the silicon wafer or by dicing it with a 3 μm grain-size blade. Dicing usually results in a better reproducibility of the facet quality, which resulted in a smaller scattering of the throughput data and therefore a better fit of the exponential decrease in throughput with channel length.

Acknowledgment. We are grateful to Dr. H. Ito from IBM Almaden Research Center in San Jose, CA, for fruitful discussions and for providing us with *N*-perfluorobenzenesulfonyloxynaphthalimide. O. J. Hagel from IMC in Linköping, Sweden, is thanked for assistance in waveguide prototype manufacturing. Ericsson Components and the National Swedish Board for Technical and Industrial Development (NUTEK) are gratefully acknowledged for providing financial support.

References and Notes

(1) (a) Booth, B. L. In *Polymers for lightwave and integrated optics: Technology and applications*; Hornak, L. A., Ed.; M. Dekker Inc.: New York, 1992; pp 231−266. (b) Hartman, D. H. In *Polymers for lightwave and integrated optics: Technology and applications*; Hornak, L. A., Ed.; M. Dekker Inc.: New York, 1992; pp 267−286.

(2) Bristow, J.; Liu, Y.; Marta, T.; Bounnak, S.; Johnson, K. *Proc. SPIE* **1995**, *2400*, 61−73.

(3) Reuter, R.; Franke, H.; Feger, C. *Appl. Opt.* **1988**, *27*, 4565−4571.

(4) Matsuura, T.; Ando, S.; Matsui, S.; Sasaki, S.; Yamamoto, F. *Electron. Lett.* **1993**, *29*, 2107−2109.

(5) Usui, M.; Imamura, S.; Sugawara, S.; Hayashida, S.; Sato, H.; Hikita, M.; Izawa, T. *Electron. Lett.* **1994**, *30*, 958−959.

(6) Maruo, Y. Y.; Sasaki, S.; Tamamura, T. *Appl. Opt.* **1995**, *34*, 1047−1052.

(7) Usui, M.; Hikita, M.; Watanabe, T.; Amano, M.; Sugawara, S.; Hayashida, S.; Immamura, S. *J. Lightwave Technol.* **1996**, *14*, 2338−2343.

(8) Chandross, E. A.; Pryde, C. A.; Tomlinson, W. J.; Weber, H. P. *Appl. Phys. Lett.* **1974**, *24*, 72−74.

(9) Kurokawa, T.; Takato, N.; Katayama, Y. *Appl. Opt.* **1980**, *19*, 3124−3129.

(10) Knoche, Th.; Müller, L.; Klein, R.; Neyer, A. *Proc. CLEO/Europe '94*, **1994**, 202−203.

(11) Fan, B.; Flagello, D. G.; Gelorme, J. D.; Oprysko, M. M.; Speth, A.;. Trewhella, J. M. European Patent 0 446 672 A1, 1991.

(12) Trewhella, J. M.; Gelorme, J. D.; Fan, B.; Speth, A.; Flagello, D.; Oprysko, M. M. *Proc. Soc. Photo-Opt. Instrum. Eng.* **1989**, *379*, 1177.

(13) Crivello, J. V. *Adv. Polym. Sci.* **1984**, *62*, 1.

(14) (a) Ito, H.; Willson, C. G. *Technical Papers of SPE Regional Technical Conference on Photopolymers*; 1980; p 207. (b) Ito, H.; Willson C. G.; Fréchet J. M. *Digest of Technical Papers of 1982 Symposium on VLSI Technology*; 1982; p 86. (c) Ito, H.; Willson C. G. *Polym. Eng. Sci.* **1983**, *23*, 1012−1018. (d) Ito, H.; Willson C. G. *ACS Symp. Ser.* **1984**, *242*, 11.

(15) Alfrey, T., Jr.; Price, C. C. *J. Polym. Sci.* **1947**, *2*, 101−106.

(16) Young, L. J. *J. Polym. Sci.* **1961**, *54*, 411−455,

(17) Pryor, W. A., Huang T.-L. *Macromolecules* **1969**, *2*, 70−77.

(18) (a) Yuki, H.; Hatada, K.; Takeshita, M. *J. Polym. Sci., Part A-1* **1969**, 667. (b) Higashimura, T.; Okamura, S.; Marishima, T.; Yonezawa, T. *J. Polym. Sci., Part B* **1969**, 23. (c) Yuki, H.; Hatada, K.; Nagata, K.; Emura, T. *Polym. J.* **1970**, *1*, 269. (d) Hatada, K.; Nagata, K.; Yuki, H. *Bull. Chem. Soc. Jpn.* **1970**, *43*, 3195. (e) Hatada, K.; Nagata, K.; Yuki, H. *Bull. Chem. Soc. Jpn.* **1970**, *43*, 3267. (f) Hatada, K.; Nagata, K.; Hasegawa, T.; Yuki, H. *Makromol. Chem.* **1977**, *178*, 2413. (g) Herman, J. J.; Teyssié, Ph. *Macromolecules* **1978**, *11*, 839.

(19) Ouano, A. C.; Carothers, J. A. Kinematics of polymer dissolution. IBM internal report, RJ1981 (27931) 4/5/77 Chemistry, IBM Research Laboratory: San Jose, CA, (Copies may be requested from: IBM Thomas J. Watson Research Center, Post Office Box 218, Yorktown Heights, NY 10598).

(20) Van Krevelen, D. W. *Properties of Polymers: Their correlation with chemical structure; Their numerical estimation and prediction from additive group contributions*, 3rd ed.; Elsevier Science Publishers: New York, 1990: (a) Chapter 6, p 138−139; (b) Chapter 6, p 148; (c) Chapter 21, p 642.

(21) Kelen, T.; Tüdös, F. *J. Macromol. Sci.—Chem.* **1975**, *A9*, 1−27. The Kelen-Tüdös linear equation is $\eta = r_1\xi - r_2/\alpha(1 - \xi)$, where r_1 and r_2 are the reactivity ratios of PFS and GMA, respectively, $\eta = G/(\alpha + F)$, $\xi = F/(\alpha + F)$, $F = x^2/y$, $G = x(y - 1)/y$, $\alpha = (F_{min}F_{max})^{-1/2}$, $x = M_1/M_2$ and $y = dM_1/dM_2$, where y is the concentration ratio of the copolymer components and M_1 and M_2 are the concentrations of PFS and GMA, respectively. From the plot of η vs ξ we obtain $r(\text{PFS}) = \eta_1$, at $\xi = 1$, and $r(\text{GMA}) = \eta_0 - /\alpha$, at $\xi = 0$.

(22) November, A. E.; Masakowski, L. M.; Hartney, M. A. *Polym. Eng. Sci.* **1986**, *26*, 1158.

(23) Tien, P. K.; Ulrich, R.; Martin, R. J. *Appl. Phys. Lett.* **1969**, *14*, 291.

(24) Robertsson, M. Internal technical report from Ericsson Components AB: A Method to Determine Refractive Index Versus Wavelength by UV−vis−NIR Reflection Interference Spectroscopy.

MA981057X